Reduced regulator dependence of neutron-matter predictions with perturbative chiral interactions

L. Coraggio,[1] J. W. Holt,[2,3] N. Itaco,[1,4] R. Machleidt,[5] and F. Sammarruca[5]

[1]*Istituto Nazionale di Fisica Nucleare, Complesso Universitario di Monte S. Angelo, Via Cintia, I-80126 Napoli, Italy*

[2]*Physik Department, Technische Universität München, D-85747 Garching, Germany*

[3]*Physics Department, University of Washington, Seattle, Washington 98195, USA*

[4]*Dipartimento di Scienze Fisiche, Università di Napoli Federico II, Complesso Universitario di Monte S. Angelo, Via Cintia, I-80126 Napoli, Italy*

[5]*Department of Physics, University of Idaho, Moscow, Idaho 83844, USA*

(Received 25 September 2012; published 17 January 2013)

We calculate the energy per particle in infinite neutron matter perturbatively using chiral N^{3}LO (next-to-next-to-next-to-leading order) two-body potentials plus N^{2}LO three-body forces. The cutoff dependence of the predictions is investigated by employing chiral interactions with different regulators. We find that the inclusion of three-nucleon forces, which are consistent with the applied two-nucleon interaction, leads to a strongly reduced regulator dependence of the results.

DOI: 10.1103/PhysRevC.87.014322 PACS number(s): 21.30.Fe, 21.65.Cd, 21.60.Jz

I. INTRODUCTION

A major breakthrough in the past decade has been the derivation of nucleon-nucleon (NN) potentials, V_{NN}, based on chiral perturbation theory (ChPT), that are able to reproduce accurately the NN data [1–3].

The idea of constructing realistic two- and three-nucleon forces (2NF and 3NF) starting from a chiral Lagrangian goes back to the seminal work of Weinberg [4–6], who invoked the concept of an effective field theory (EFT) to study the S matrix for processes involving arbitrary numbers of low-momentum pions and nucleons. In this approach, the long-range forces are ruled by the symmetries of low-energy QCD (particularly, spontaneously broken chiral symmetry), and the short-range dynamics is absorbed into a complete basis of contact terms that are proportional to low-energy constants (LECs) fit to two-nucleon (2N) data.

One great advantage of ChPT is that it generates nuclear two- and many-body forces on an equal footing [3,7,8]. Most interaction vertices that appear in the 3NF and in the four-nucleon force (4NF) also occur in the 2NF. The parameters carried by these vertices are fixed (along with the LECs of the 2N contact terms) in the construction of the chiral 2NF. Consistency then requires that for the same vertices the same parameter values are used in the 2NF, 3NF, 4NF, and so on.

A crucial theme in EFT is regulator independence within the range of validity of the theory. In other words, the physical observables calculated in the theory must be independent of both the choice of the regulator function and its cutoff scale Λ. ChPT is a low-momentum expansion which is valid only for momenta $Q < \Lambda_\chi \simeq 1$ GeV, where Λ_χ denotes the chiral symmetry-breaking scale. Therefore, NN potentials derived in this framework are usually multiplied by a regulator function

$$f(p', p) = \exp[-(p'/\Lambda)^{2n} - (p/\Lambda)^{2n}], \qquad (1)$$

where typical choices for the cutoff parameter are $\Lambda \simeq 0.5$ GeV. In regards to the physics of the two-nucleon problem, it is obvious that the solutions of the Lippmann-Schwinger equation, that are related to the two-nucleon observables, may depend sensitively on the regulator and its cutoff parameter. This unwanted dependence is then removed by a renormalization procedure, in which the contact terms are readjusted to reproduce the two-nucleon phase shifts and data. However, it is well known that phase equivalent potentials do not necessarily yield identical results in the many-body problem. Thus, one may be confronted with cutoff dependence in the many-body system [9]. However, in the many-body problem, 3NF, 4NF, and so on also contribute, which will have impact on the final predictions and may either increase or reduce the cutoff dependence.

A convenient theoretical laboratory to investigate this issue is infinite nuclear matter and neutron matter. The advantage of pure neutron matter is that the contact interaction, V_E, and the 1π-exchange term, V_D, that appear in the next-to-next-to-leading order (N^{2}LO) three-body force vanish [10]. Thus, the low-energy constants of V_E and V_D (known as c_E and c_D), which cannot be constrained by two-body observables, are not needed. Consequently, the calculation of the ground-state energy of infinite neutron matter, with chiral 3NFs up to N^{2}LO, depends only on parameters that have been fixed in the two-nucleon system.

We note that there have been already some attempts to study the uncertainties in neutron-matter predictions using chiral forces, e.g., by Hebeler and Schwenk [10] and Tews *et al.* [11], who come up with uncomfortably large uncertainties for reasons to be discussed below. It is also worth noting that, aside from the above considerations, neutron matter, and more generally isospin-asymmetric nuclear matter, is currently of great interest in the nuclear physics community because of its close connection with the physics of neutron-rich nuclei and, for higher densities, with the structure of neutron stars.

It is the purpose of the present paper to investigate how the equation of state of neutron matter, calculated using chiral nuclear potentials, depends on the choice of the regulator function. More precisely, we employ three different chiral potentials whose cutoff parameters are $\Lambda = 414$ [12], 450, and 500 MeV [1,3] and calculate, including 3NF effects, the energy per nucleon for neutron matter at nuclear densities in

the framework of many-body perturbation theory. The crucial point of our calculations is that we use in the 3NF exactly the same LECs as well as the same cutoff parameters as in the 2NF. We will show that this consistent use of the LECs in the 2NF *and* 3NF leads to a substantial reduction of the regulator dependence of the neutron-matter predictions.

The paper is organized as follows. In Sec. II, we briefly describe the features of the different chiral potentials employed and, in Sec. III, we give an outline of the calculation of the energy per nucleon in neutron matter that takes into account 3NF effects. Our results are presented in Sec. IV, and some concluding remarks and an outlook are given in Sec. V.

II. THE CHIRAL POTENTIALS

During the past two decades, it has been demonstrated that chiral effective field theory (chiral EFT) is a powerful tool to deal with hadronic interactions at low energy in a systematic and model-independent way (see Refs. [3,13] for recent reviews). For the construction of an EFT, it is crucial to identify a separation of scales. In the hadron spectrum, a large gap between the masses of the pions and the masses of the vector mesons, like $\rho(770)$ and $\omega(782)$, can clearly be identified. Thus, it is natural to assume that the pion mass sets the soft scale, $Q \sim m_\pi$, and the ρ mass the hard scale, $\Lambda_\chi \sim m_\rho \sim 1$ GeV, also known as the chiral-symmetry-breaking scale. This is suggestive of considering a low-energy expansion arranged in terms of the soft scale over the hard scale, $(Q/\Lambda_\chi)^\nu$, where Q is generic for an external momentum (nucleon three-momentum or pion four-momentum) or a pion mass. The appropriate degrees of freedom are, obviously, pions and nucleons, not quarks and gluons. For this EFT to rise above the level of phenomenology, it must have a firm link with QCD. The link is established by having the EFT observe all relevant symmetries of the underlying theory, in particular, the broken chiral symmetry of low-energy QCD [4]. The past 15 years have seen great progress in applying ChPT to nuclear forces. As a result, NN potentials of high precision have been constructed, which are based upon ChPT carried to N^{3}LO.

Since ChPT is a low-momentum expansion, valid only for momenta $Q < \Lambda_\chi$, the potentials are either abruptly set to zero for momenta above a certain cutoff $\Lambda < \Lambda_\chi$ ("sharp cutoff") or they are multiplied with a smooth regulator function, like, e.g., the one of Gaussian shape given in Eq. (1).

In this investigation, we consider three N^{3}LO potentials which differ by the cutoff parameter Λ and/or the regulator function:

(i) $\Lambda = 414$ MeV together with a sharp cutoff (published in Ref. [12]).
(ii) $\Lambda = 450$ MeV using the regulator function Eq. (1) with $n = 3$. We have constructed this potential for the present investigation.
(iii) $\Lambda = 500$ MeV using the regulator function Eq. (1) with $n = 2$ for the 2π exchange contributions. This potential was published in 2003 [1].

All three potentials use the same (comprehensive) analytic expressions which can be found in Ref. [3]. Note that the Gaussian regulator function Eq. (1) suppresses the potential also for $Q < \Lambda$, which is why we use a sharp cutoff function in the case of the lowest cutoff of 414 MeV. Cutoff independence is an important aspect of an EFT. In lower partial waves, the cutoff dependence of the NN phase shifts is counterbalanced by an appropriate adjustment of the contact terms which, at N^{3}LO, contribute in S, P, and D waves. The extent to which cutoff independence can be achieved in lower partial waves is demonstrated in Figs. 1 and 2. In F and higher partial waves (where there are no NN contact terms) the LECs of the dimension-two πN Lagrangian can be used to obtain cutoff independence of the phase shift predictions; see Table I and Fig. 3.

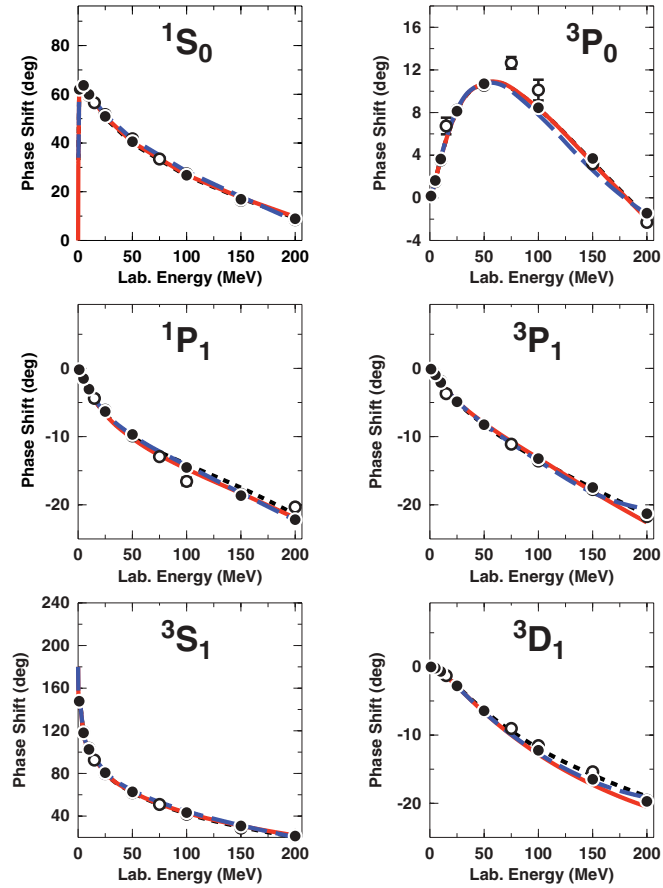

FIG. 1. (Color online) Neutron-proton phase parameters as predicted by chiral N^{3}LO potentials with different cutoff scale Λ. Solid (red) curve, $\Lambda = 414$ MeV; dashed (blue) curve, $\Lambda = 450$ MeV; and dotted (black) curve, $\Lambda = 500$ MeV. Partial waves with total angular momentum $J \leqslant 1$ are displayed. The solid dots and open circles are the results from the Nijmegen multienergy np phase shift analysis [14] and the VPI/GWU single-energy np analysis SM99 [15], respectively.

An important advantage of the EFT approach to nuclear forces is that it creates two- and many-body forces on an equal footing. The first nonvanishing 3NF occurs at N^{2}LO. At this order, there are three 3NF topologies: the two-pion exchange (2PE), one-pion exchange (1PE), and 3N-contact interactions. The 2PE 3N-potential is given by

$$V_c = \left(\frac{g_A}{2f_\pi}\right)^2 \frac{1}{2} \sum_{i\neq j\neq k} \frac{(\vec{\sigma}_i \cdot \vec{q}_i)(\vec{\sigma}_j \cdot \vec{q}_j)}{(q_i^2 + m_\pi^2)(q_j^2 + m_\pi^2)} F_{ijk}^{ab} \tau_i^a \tau_j^b \quad (2)$$

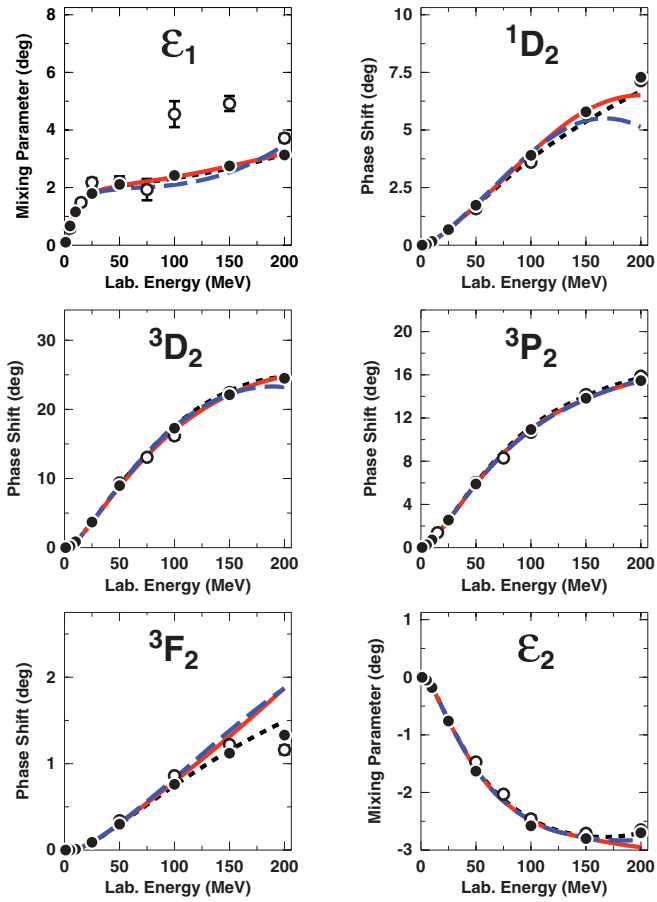

FIG. 2. (Color online) Same as Fig. 1, but $J = 2$ phase shifts and $J \leqslant 2$ mixing parameters are shown.

with $\vec{q}_i \equiv \vec{p}_i{}' - \vec{p}_i$, where $\vec{p}_i$ and $\vec{p}_i{}'$ are the initial and final momenta of nucleon i, respectively, and

$$F_{ijk}^{ab} = \delta^{ab}\left[-\frac{4c_1 m_\pi^2}{f_\pi^2} + \frac{2c_3}{f_\pi^2}\,\vec{q}_i \cdot \vec{q}_j\right] + \frac{c_4}{f_\pi^2}\sum_c \epsilon^{abc}\,\tau_k^c\,\vec{\sigma}_k \cdot [\vec{q}_i \times \vec{q}_j]. \quad (3)$$

Note that the 2PE 3NF does not contain any new parameters, because the LECs c_1, c_3, and c_4 appear already in the 2PE 2NF.

TABLE I. For the various chiral N^{3}LO NN potentials used in the present investigation, we show the cutoff Λ, the type of regulator, the exponent n used in the regulator function, Eq. (1), and the LECs of the dimension-two πN Lagrangian, c_i (in units of GeV^{-1}), which are relevant for the N^{2}LO 3NF in neutron matter.

	Cutoff parameter Λ (MeV)		
	414	450	500
Regulator type	Sharp	Gaussian	Gaussian
n		3	2
c_1	−0.81	−0.81	−0.81
c_3	−3.00	−3.40	−3.20

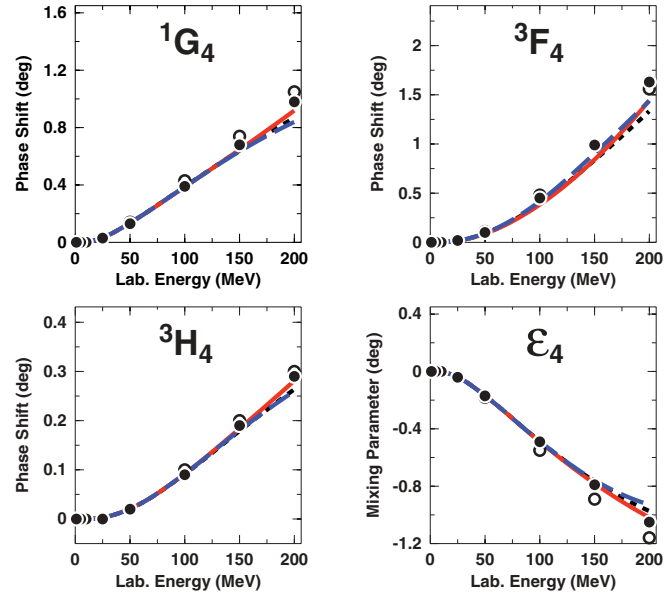

FIG. 3. (Color online) Same as Fig. 1, but some representative peripheral partial waves are shown.

The 1PE contribution is

$$V_D = -\frac{c_D}{f_\pi^2 \Lambda_\chi}\,\frac{g_A}{8 f_\pi^2}\sum_{i\neq j\neq k}\frac{\vec{\sigma}_j \cdot \vec{q}_j}{q_j^2 + m_\pi^2}(\boldsymbol{\tau}_i \cdot \boldsymbol{\tau}_j)(\vec{\sigma}_i \cdot \vec{q}_j) \quad (4)$$

and the 3N contact potential reads

$$V_E = \frac{c_E}{f_\pi^4 \Lambda_\chi}\,\frac{1}{2}\sum_{j\neq k}\boldsymbol{\tau}_j \cdot \boldsymbol{\tau}_k. \quad (5)$$

In the above, we use $g_A = 1.29$, $f_\pi = 92.4$ MeV, $m_\pi = 138.04$ MeV, and $\Lambda_\chi = 700$ MeV. The last two 3NF terms involve the two new parameters c_D and c_E, which do not appear in the 2N problem. There are many ways to pin these two parameters down. The triton binding energy and the nd doublet scattering length $^2a_{nd}$ can be used. Alternatively, one may choose the binding energies of ^{3}H and ^{4}He or an optimal overall fit of the properties of light nuclei. However, in neutron matter, V_D and V_E do not contribute such that we do not have to worry about their values here. Note also that the c_4 term of V_c, Eqs. (2) and (3), vanishes in neutron matter.

III. CALCULATION OF THE ENERGY PER PARTICLE IN NEUTRON MATTER

We calculate the ground-state energy per particle (g.s.e.) of infinite neutron matter within the framework of many-body perturbation theory. In particular, we express the g.s.e. as a sum of Goldstone diagrams up to third order.

In order to take into account the effects of the N^{2}LO 3NF, a density-dependent two-body potential $\overline{V}_{NNN}$ is added to the chiral N^{3}LO potential V_{NN}. This potential $\overline{V}_{NNN}$ is obtained by summing one nucleon over the filled Fermi sea, which leads to a density-dependent two-nucleon interaction [16,17]. Hebeler *et al.* [10] have pointed out that to take care of the correct combinatorial factors of the normal ordering at the two-body level of the 3NF, the matrix elements of $\overline{V}_{NNN}(k_F)$

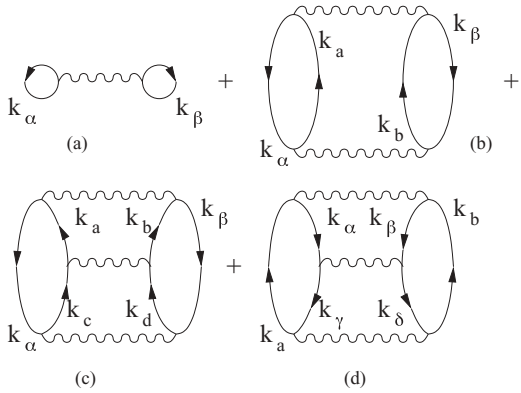

FIG. 4. First-, second-, and third-order diagrams of the Goldstone expansion included in our calculations with V_{NN} vertices only. Latin-letter subscripts denote particle states, and Greek-letter subscripts correspond to hole states.

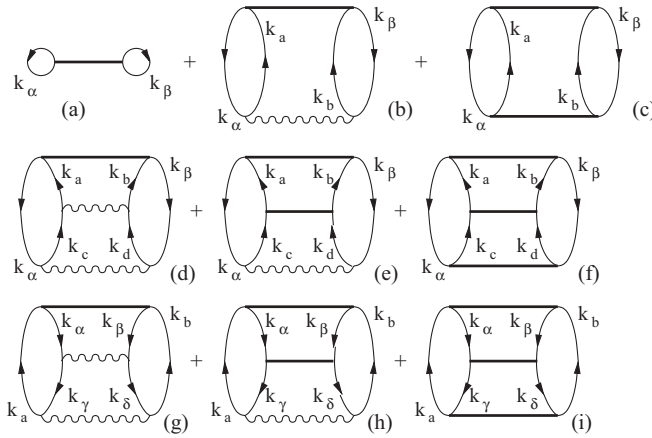

FIG. 5. Same as in Fig. 4, but also including $\overline{V}_{NNN}$ vertices, which are denoted with thick straight lines.

are to be multiplied by a factor of 1/3 in the first-order Hartree-Fock (HF) diagram and by a factor of 1/2 in the calculation of the single-particle energies (s.p.e.).

In Fig. 4 we show the diagrams we have included in our calculation, where only the V_{NN} vertices are taken into account. The only diagram we do not include is the third-order *ph* diagram. The diagrams that include the effects of V_{NNN} are shown in Fig. 5.

The first-order HF contribution is explicitly given by

$$E_1 = \frac{8}{\pi}\int_0^{k_F} k^2 dk \left[1 - \frac{3}{2}\frac{k}{k_F} + \frac{1}{2}\left(\frac{k}{k_F}\right)^3\right] \sum_{JLS}(2J+1)\left[V_{NN}^{JLLS}(k,k) + \frac{1}{3}\overline{V}_{NNN}^{JLLS}(k,k)\right]. \tag{6}$$

The second-order diagrams are computed using the so-called angle-average (AA) approximation [18], and their contribution is

$$E_2 = -\frac{6}{\pi^2 k_F^3}\int_0^{2k_F} K^2 dK \int_0^{\infty} k'^2 dk' \int_0^{\infty} k^2 dk P(k',K)Q(k,K) \sum_{JL\bar{L}S}(2J+1)\frac{\left[V_{NN}^{JL\bar{L}S}(k,k') + \overline{V}_{NNN}^{JL\bar{L}S}(k,k')\right]^2}{E(k,k',K)}. \tag{7}$$

The operators P and Q are defined through the relationships

$$\begin{aligned}
Q(k,K) &= 0, \quad 0 \leqslant k \leqslant \left(k_F^2 - \frac{K^2}{4}\right)^{1/2} \\
&= -\frac{k_F^2 - k^2 - K^2/4}{kK}, \quad \left(k_F^2 - \frac{K^2}{4}\right)^{1/2} \leqslant k \leqslant \left(k_F + \frac{K}{2}\right) \\
&= 1, \quad k \geqslant \left(k_F + \frac{K}{2}\right) \\
P(k,K) &= 1, \quad 0 \leqslant k \leqslant \left(k_F - \frac{K}{2}\right) \\
&= \frac{k_F^2 - k^2 - K^2/4}{kK}, \quad \left(k_F - \frac{K}{2}\right) \leqslant k \leqslant \left(k_F^2 - \frac{K^2}{4}\right)^{1/2} \\
&= 0, \quad k \geqslant \left(k_F^2 - \frac{K^2}{4}\right)^{1/2}.
\end{aligned}$$

In Eq. (7), the denominator is $E(k,k',K) = \frac{\hbar^2 k'^2}{M} + 2U(\sqrt{\frac{K^2}{4}+k'^2}) - \frac{\hbar^2 k^2}{M} - 2U(\sqrt{\frac{K^2}{4}+k^2})$, with $U(\tilde{k})$ being the self-consistent single-particle potential:

$$U(\tilde{k}) = 8\sum_{JLLS}(2J+1)^2 \left\{\left[\int_0^{\frac{1}{2}(k_F-\tilde{k})} \tilde{k}'^2 d\tilde{k}' + \frac{1}{2\tilde{k}}\int_{\frac{1}{2}(k_F-\tilde{k})}^{\frac{1}{2}(k_F+\tilde{k})} \tilde{k}' d\tilde{k}' \left(\frac{1}{4}\left(k_F^2 - \tilde{k}^2\right) - \tilde{k}'(\tilde{k}' - \tilde{k})\right)\right] \times \left[V_{NN}^{JLLS}(\tilde{k}',\tilde{k}') + \frac{1}{2}\overline{V}_{NNN}^{JLLS}(\tilde{k}',\tilde{k}')\right]\right\}. \tag{8}$$

The particle-particle (pp) and hole-hole (hh) third-order diagrams are also computed in the AA approximation, and their explicit expressions are

$$E_3(\mathrm{pp}) = \frac{12}{(\pi k_F)^3}\int_0^{2k_F} K^2 dK \int_0^\infty k^2 dk \int_0^\infty k'^2 dk' \int_0^\infty k''^2 dk'' P(k,K)Q(k',K)Q(k'',K) \sum_{JL\overline{L}\overline{L}'S} (2J+1)$$
$$\times \left[V_{NN}^{JL\overline{L}S}(k,k') + \overline{V}_{NNN}^{JL\overline{L}S}(k,k')\right]\left[V_{NN}^{J\overline{L}\overline{L}'S}(k',k'') + \overline{V}_{NNN}^{J\overline{L}\overline{L}'S}(k',k'')\right]\left[V_{NN}^{J\overline{L}'LS}(k'',k) + \overline{V}_{NNN}^{J\overline{L}'LS}(k'',k)\right]/[E(k'',k)\cdot E(k',k)], \quad (9)$$

$$E_3(\mathrm{hh}) = \frac{2}{(\pi k_F)^3}\int_0^{2k_F} K^2 dK \int_0^\infty k^2 dk \int_0^\infty k'^2 dk' \int_0^\infty k''^2 dk'' P(k,K)Q(k',K)P(k'',K)$$
$$\times \sum_{JL\overline{L}\overline{L}'S} (2J+1)\left[V_{NN}^{JL\overline{L}S}(k,k') + \overline{V}_{NNN}^{JL\overline{L}S}(k,k')\right]\left[V_{NN}^{J\overline{L}\overline{L}'S}(k',k'') + \overline{V}_{NNN}^{J\overline{L}\overline{L}'S}(k',k'')\right]$$
$$\times \left[V_{NN}^{J\overline{L}'LS}(k'',k) + \overline{V}_{NNN}^{J\overline{L}'LS}(k'',k)\right]/[E(k',k'')\cdot E(k',k)]. \quad (10)$$

We have also calculated the [2|1] Padé approximant [19]

$$E_{[2|1]} = E_0 + E_1 + \frac{E_2}{1 - E_3/E_2}, \quad (11)$$

E_i being the ith-order energy contribution in the perturbative expansion of the g.s.e. The Padé approximant is an estimate of the value to which the perturbative series may converge. Thus, the comparison between the third-order results and those obtained by means of the [2|1] Padé approximant provides an indication of the size of the higher-order perturbative terms. It is worth mentioning that the role of Padé approximants in many-body perturbation theory for nuclear systems has been explored in the past decade for finite nuclei [20–23].

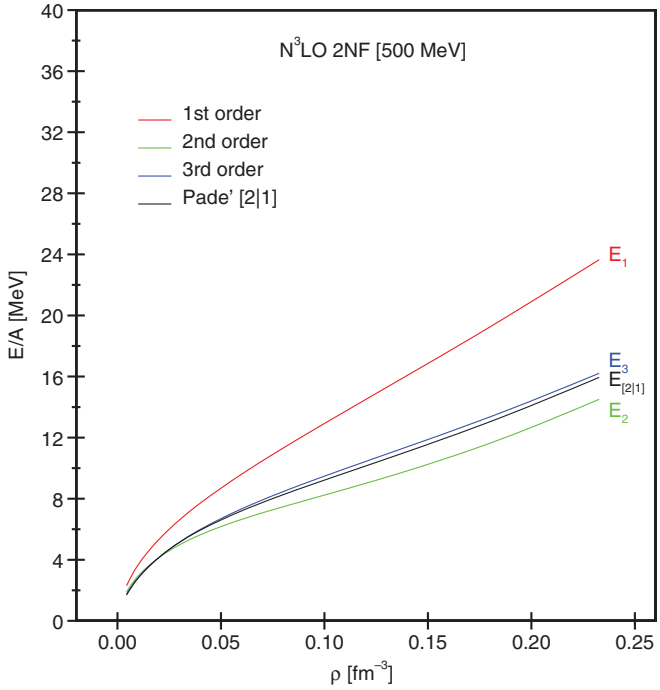

FIG. 6. (Color online) Neutron-matter energy per particle obtained from the N^{3}LO 2NF with cutoff $\Lambda = 500$ MeV. The first, second, and third order in the perturbative expansion and the Padé approximant [2|1] are shown as a function of density ρ.

IV. RESULTS

As explained in the previous section, we calculate the energy per particle of neutron matter in the framework of many-body perturbation theory, including contributions up to third order in the interaction. Therefore, it is of interest to obtain an idea of the convergence of the perturbative expansion of the g.s.e.

In Fig. 6, we show the neutron-matter energy per nucleon as a function of density, calculated at various orders in the perturbative expansion by applying the chiral N^{3}LO NN potential with a cutoff parameter equal to 500 MeV. We have chosen here the potential with the largest cutoff since it has the worst perturbative behavior. From the inspection of Fig. 6, it can be seen that the energy per nucleon calculated at second order, E_2, does not differ much from the one computed at third order, E_3, for the whole range of densities shown. The perturbative character is also indicated by the fact that E_3 is quite close to the energy obtained with the [2|1] Padé approximant.

For completeness, we mention that we also performed calculations employing the chiral N^{3}LO NN potential with a cutoff parameter equal to 600 MeV [3], but we found its perturbative behavior unsatisfactory, in agreement with the observations by Tews *et al.* [11].

We have also investigated the perturbative behavior of our calculations when including the effects of V_{NNN}. Figure 7 shows that, starting from the same N^{3}LO potential, there is a small enhancement of the higher-order terms when including the N^{2}LO 3NF. Nevertheless, the results at third order are very close to those obtained with the [2|1] Padé approximant.

Our main goal is to calculate the g.s.e. per particle in infinite neutron matter, starting from N^{3}LO chiral NN potentials that apply different regulator functions. This is done by using the chiral potentials introduced in Sec. II. We have added to each 2NF a chiral N^{2}LO 3NF whose low-energy constants c_1

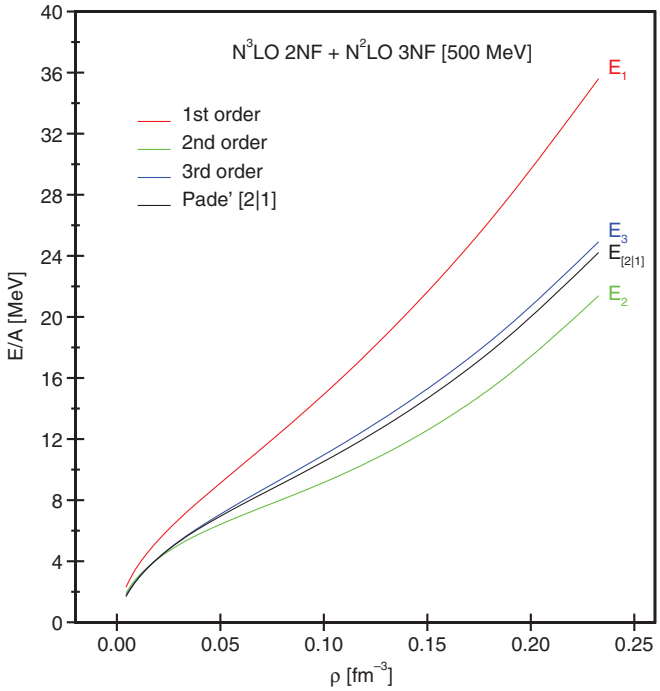

FIG. 7. (Color online) Same as in Fig. 6, but including the contribution of the N^{2}LO 3NF.

and c_3, cutoff parameters, and regulator function are exactly the same as in the corresponding N^{3}LO NN potential; see Table I.

In Fig. 8, we show our results, obtained at third order in the perturbative expansion, with and without taking into account

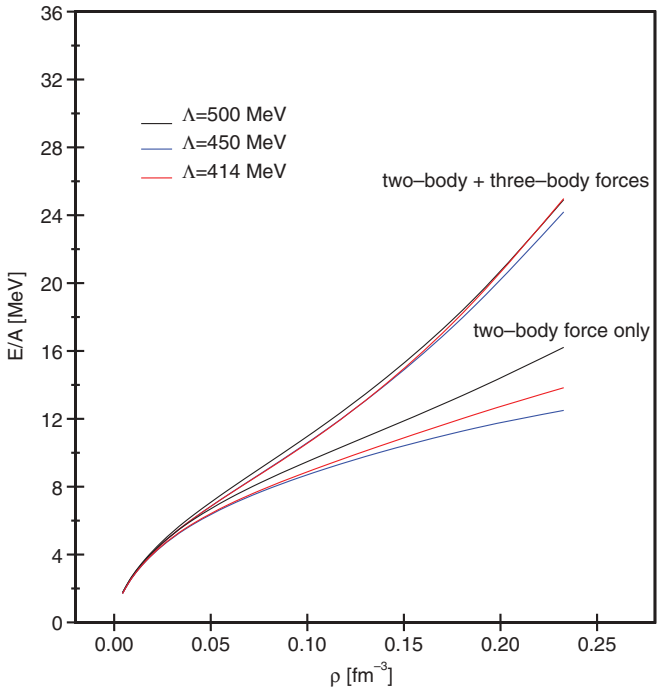

FIG. 8. (Color online) Results obtained for the g.s.e. per particle of infinite neutron matter at third-order in perturbation theory for three sets of chiral interactions which differ by the cutoff Λ.

3NF effects. The results obtained with 2NFs show considerable dependence on the choice of the regulator and its cutoff parameter. This is at variance with the desired regulator independence of the EFT. However, when including the contributions of the three-body potentials, which are consistent with their 2NF partner, regulator dependence is strongly reduced. This is our main result and first clear evidence that modern chiral potentials can provide model-independent results in many-body calculations *if 2NF and 3NF are treated consistently.*

V. CONCLUDING REMARKS AND OUTLOOK

In this paper we have studied the regulator dependence of many-body predictions when employing chiral two- and three-nucleon potentials, using as a testing ground the perturbative calculation of the neutron-matter energy per particle. We find substantial regulator dependence of the predictions when only 2NFs are taken into account. The main outcome of this study is the observation that the 3NF can play a crucial role in the restoration of regulator independence. However, this mechanism works properly only when the chiral 2NF and 3NF are treated consistently in the sense that the same parameters are used for the same vertices that occur in all topologies involved. This is particularly true for the LECs c_1 and c_3 occurring first at N^{2}LO in the chiral power counting.

In Refs. [10,11] the large uncertainties of the results for the ground-state energy per neutron trace back to the choice of using a range of values for c_1 and c_3 obtained from a high-order analysis of πN scattering [24]. This is at variance with the c_is employed in the present paper which, as reported in Sec. II, are uniquely fixed in peripheral NN partial waves.

In closing, we note that the present investigation deals only with identical nucleon systems and that the regulator dependence should also be investigated in systems with different concentrations of interacting protons and neutrons. In infinite symmetric nuclear matter, contributions from the intermediate-range 1π-exchange component V_D and the short-range contact interaction V_E also come into play. This means that the calculation of the g.s.e. depends also on the coupling constants c_D and c_E. Even though these parameters can be fixed in few-body systems, there is some freedom in doing so, resulting in more latitude for the 3NF contribution in nuclear matter (as compared to pure neutron matter).

This will be an interesting subject for a future study that may shed more light on the topic of regulator independence of many-body calculations with chiral potentials. The results of such investigations will provide valuable guidance for the proper application of these interactions in microscopic nuclear structure calculations.

ACKNOWLEDGMENTS

This work was supported in part by the US Department of Energy under Grants No. DE-FG02-03ER41270 and No. DE-FG02-97ER-41014, by the Italian Ministero dell'Istruzione, dell'Università e della Ricerca (MIUR) under PRIN 2009, by BMBF (the DFG cluster of excellence: Origin and Structure of the Universe), and by DFG and NSFC (CRC110).

[1] D. R. Entem and R. Machleidt, Phys. Rev. C **68**, 041001(R) (2003).
[2] E. Epelbaum, W. Glöckle, and U.-G. Meißner, Nucl. Phys. A **747**, 362 (2005).
[3] R. Machleidt and D. R. Entem, Phys. Rep. **503**, 1 (2011).
[4] S. Weinberg, Physica A **96**, 327 (1979).
[5] S. Weinberg, Phys. Lett. B **251**, 288 (1990).
[6] S. Weinberg, Nucl. Phys. B **363**, 3 (1991).
[7] S. Weinberg, Phys. Lett. B **295**, 114 (1992).
[8] U. van Kolck, Phys. Rev. C **49**, 2932 (1994).
[9] L. Coraggio, A. Covello, A. Gargano, N. Itaco, and T. T. S. Kuo, Ann. Phys. **327**, 2125 (2012).
[10] K. Hebeler and A. Schwenk, Phys. Rev. C **82**, 014314 (2010).
[11] I. Tews, T. Krüger, K. Hebeler, and A. Schwenk, arXiv:1206.0025v2 [nucl-th].
[12] L. Coraggio, A. Covello, A. Gargano, N. Itaco, D. R. Entem, T. T. S. Kuo, and R. Machleidt, Phys. Rev. C **75**, 024311 (2007).
[13] E. Epelbaum, H.-W. Hammer, and U.-G. Meißner, Rev. Mod. Phys. **81**, 1773 (2009).
[14] V. G. J. Stoks, R. A. M. Klomp, M. C. M. Rentmeester, and J. J. de Swart, Phys. Rev. C **48**, 792 (1993).
[15] R. A. Arndt, I. I. Strakovsky, and R. L. Workman, SAID, Scattering Analysis Interactive Dial-In Computer Facility, George Washington University, solution SM99 (summer 1999); for more information see, e.g., R. A. Arndt, I. I. Strakovsky, and R. L. Workman, Phys. Rev. C **50**, 2731 (1994).
[16] J. W. Holt, N. Kaiser, and W. Weise, Phys. Rev. C **79**, 054331 (2009).
[17] J. W. Holt, N. Kaiser, and W. Weise, Phys. Rev. C **81**, 024002 (2010).
[18] E. L. Lomon and M. McMillan, Ann. Phys. (NY) **23**, 439 (1963).
[19] G. A. Baker and J. L. Gammel, *The Padé Approximant in Theoretical Physics*, Mathematics in Science and Engineering Vol. 71 (Academic Press, New York, 1970).
[20] L. Coraggio, A. Covello, A. Gargano, N. Itaco, and T. T. S. Kuo, Phys. Rev. C **73**, 014304 (2006).
[21] L. Coraggio, A. Covello, A. Gargano, N. Itaco, and T. T. S. Kuo, Phys. Rev. C **75**, 057303 (2007).
[22] R. Roth and J. Langhammer, Phys. Lett. B **683**, 272 (2010).
[23] J. Langhammer, R. Roth, and C. Stumpf, Phys. Rev. C **86**, 054315 (2012).
[24] H. Krebs, A. Gasparyan, and E. Epelbaum, Phys. Rev. C **85**, 054006 (2012).